arXiv:hep-ex/0011098v2 19 Sep 2001

Differential Cross Section Measurement of η Photoproduction on the Proton from Threshold to 1100 MeV

F. Renard [a], M. Anghinolfi [b], O. Bartalini [c], V. Bellini [d], J.P. Bocquet [a], M. Capogni [c], M. Castoldi [b], P. Corvisiero [b], A. D'Angelo [c], J.-P. Didelez [e], R. Di Salvo [c], C. Gaulard [f], G. Gervino [g], F. Ghio [h], B. Girolami [h], M. Guidal [e], E. Hourany [e], V. Kouznetsov [i], R. Kunne [e], A. Lapik [i], P.Levi Sandri [f], A. Lleres [a], D. Morriciani [c], V. Nedorezov [i], L. Nicoletti [c,a], D. Rebreyend [a,1], N. Rudnev [j], M. Sanzone [b] C. Schaerf [c], M.-L. Sperduto [d], M.-C. Sutera [d], M. Taiuti [b] A. Turinge [k], Q. Zhao [e], A. Zucchiatti [b]

GRAAL Collaboration

[a] *IN2P3, Institut des Sciences Nucléaires, 38026 Grenoble, France*

[b] *INFN sezione di Genova and Università di Genova, 16146 Genova, Italy*

[c] *INFN sezione di Roma II and Università di Roma "Tor Vergata", 00133 Roma, Italy*

[d] *INFN sezione di Catania and Università di Catania, 95100 Catania,Italy*

[e] *IN2P3, Institut de Physique Nucléaire, 91406 Orsay, France*

[f] *INFN Laboratori Nazionali di Frascati, 00044 Frascati, Italy*

[g] *INFN sezione di Torino and Università di Torino, 10125 Torino, Italy*

[h] *INFN sezione di Roma I and Istituto Superiore di Sanità, 00161 Roma, Italy*

[i] *Institute for Nuclear Research, 117312 Moscow, Russia*

[j] *Institute of Theoretical and Experimental Physics, 117259 Moscow, Russia*

[k] *RRC "Kurchatov Institute", 123182 Moscow, Russia*

Abstract

The differential cross section for the reaction $p(\gamma,\eta p)$ has been measured from threshold to 1100 MeV photon laboratory energy. For the first time, the region of the $S_{11}(1535)$ resonance is fully covered in a photoproduction experiment and allows a precise extraction of its parameters at the photon point. Above 1000 MeV, S-wave

dominance vanishes while a P-wave contribution is observed whose nature will have to be clarified. These high precision data together with the already measured beam asymmetry data will provide stringent constraints on the extraction of new couplings of baryon resonances to the η meson.

PACS: 13.60.Le, 13.88.+e, 14.20.Gk, 25.20.Lj

Key words: eta photoproduction, differential cross section, polarization observables, photon beam asymmetry, baryon resonances.

The nucleon, like any composite object, shows a spectrum of excited states intimately connected to its internal structure. Precise measurements of the properties of these states offer a unique opportunity to test Quantum ChromoDynamics (QCD) in the non-perturbative regime and to approach the confinement problem. Historically, they have been first observed as baryon resonances in π-N scattering [1], with a rich spectrum typical of a few-body problem. Since the dominant decay channel of nucleon resonances is the strong decay through meson emission, photoproduction of light mesons (π, η, K,...) gives a complementary way to access information about nucleon spectroscopy. Whereas elastic and inelastic π-N scattering have provided precise values for the masses and widths [2], meson photoproduction allows a measurement of the electromagnetic transitions, thus provides a stringent dynamical test for models of the nucleon.

Among the large variety of existing models [3], Constituent Quark Models (CQM) have been the most successful in accounting for the observed spectrum. These "QCD-inspired" models describe the nucleon as three massive constituent quarks ($m_Q \approx$300 MeV/c^2) confined by a harmonic potential. The hyperfine interaction, essential to reproduce the spectrum, is derived from gluon exchange in the original approach, or meson exchange in the more recent chiral version of CQM [1]. Both versions also predict so far unobserved states ("missing resonances") whose absence has been interpreted, for instance, by a weak coupling to π-N channels [4].

Extraction of resonance properties in pion photoproduction is a difficult exercise since one needs to disentangle many overlapping contributions [5,6]. By contrast, eta photoproduction close to threshold is strongly dominated by a single resonance, the $S_{11}(1535)$, and thus is the ideal place to investigate this benchmark state for nucleon models. Analyses of the available data base, including differential cross sections below 800 MeV [7], target asymmetries below 1000 MeV [8] and our beam asymmetry Σ measurements [9] have identified two other resonances : the $D_{13}(1520)$ and the $F_{15}(1680)$. On the one hand, Σ

[1] E-mail address: rebreyend@isn.in2p3.fr

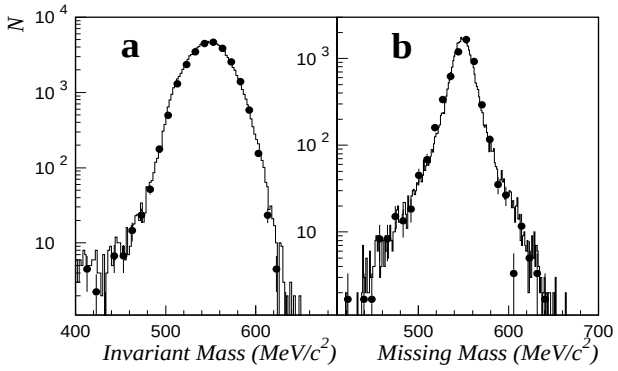

Fig. 1. a: Invariant mass spectrum for $\eta \to 2\gamma$ decay. b: Missing mass spectrum, as calculated from the proton momentum. Data (full curve) and simulation (black dots) are presented with all kinematical cuts applied.

was shown to be very sensitive to the D_{13} and allowed a precise extraction of its parameters [10–13]. On the other hand, the $F_{15}(1680)$ was suggested to explain the forward peaking observed in Σ above 1000 MeV, but, in the absence of cross section data at this energy, no definite conclusion could be reached.

In this paper, we report on measurements of the differential cross section and extraction of the total cross section for the reaction $p(\gamma, \eta p)$ from threshold E_γ=707 MeV (W=1485 MeV) to 1100 MeV (W=1716 MeV), where W is the total CM energy.

These data have been obtained with the GRAAL facility, located at the ESRF (European Synchrotron Radiation Facility) in Grenoble. The polarized and tagged photon beam is created by Compton backscattering of laser light from the 6.04 GeV electrons circulating in the storage ring. The measurements presented here used the green line (λ=514 nm) of an Argon laser; the γ-ray energy spectrum extends from 500 MeV (geometrical limit of the tagging system) to the Compton edge at 1100 MeV. Detailed description of the beam, 4π detector characteristics and acquisition system can be found in refs. [9,14–17]. An energy deposition in the BGO calorimeter larger than 180 MeV in coincidence with an electron in the tagging system, triggers the data acquisition and allows simultaneous recording of the $\pi^0 p$ and ηp channels.

Complete detection of the reaction products is required in the event analysis. The photons from neutral η decays ($\eta \to 2\gamma$ and $\eta \to 3\pi^0 \to 6\gamma$) are identified in the BGO calorimeter, while the recoil proton is tracked in wire chambers and characterized by time of flight (ToF) and dE/dx measurements. With the tagger providing the energy of the incoming photon, the kinematics is overdetermined and a clean event selection is easily achieved using kinematical cuts (6 in total). Two examples are given with the invariant mass of the η (Fig. 1-a) and the missing mass calculated from the proton momentum

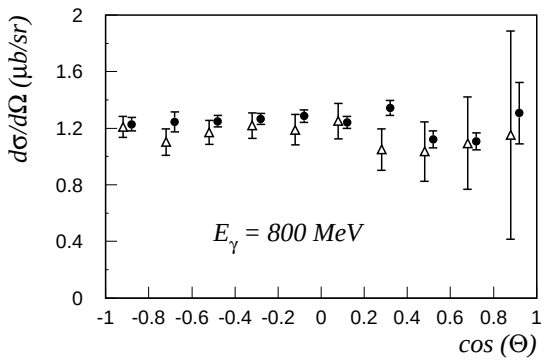

Fig. 2. Differential cross section for the $p(\gamma, \eta p)$ reaction at 800 MeV. Results for events with $\eta \to 2\gamma$ (black dot) and $\eta \to 3\pi^0$ (open triangles) decays are compared.

(Fig. 1-b). For both quantities, the simulated spectrum nicely reproduces the experimental shape, which indicates the reliability of the simulation program and the absence of any electromagnetic background. The average hadronic background has been estimated to be less than 1% [16].

The cross section normalization takes into account the target thickness, the photon beam intensity, the detection efficiency and the branching ratios of the η-meson decays taken from [2] ($\eta \to 2\gamma$: 39.21±0.34 %, $\eta \to 3\pi^0$: 32.2±0.4 %). The thickness of the liquid hydrogen target is 0.217±0.003 g·cm^{-2}, which gives a contribution of 1.5% to the systematic errors. Empty target runs have indicated a contribution of the target walls of 0.9%, consistent with their thickness. The photon intensity is monitored by thin plastic scintillators located between the target and a total absorption calorimeter (Spacal) which serves as a beam dump. Both detectors are in coincidence with the tagging system and their ToF spectra are measured for correction of accidentals. The low efficiency of the thin monitor ($\simeq 2.7\%$) prevents pile-up effects at high photon rate and is measured by comparison with the Spacal rate at low flux.

The detector efficiency (50% on average) is calculated with a complete Monte-Carlo simulation of the apparatus, including the dependence of beam shape on energy and polarization, using a realistic event generator [18]. Apart from the geometrical acceptance, the main loss comes from the overlap of clusters associated with γ-rays in the BGO ball (4 crystals hit on average per photon). This effect is strongly correlated to the γ-ray multiplicity as well as the cluster threshold, and is, moreover, energy dependent. In order to test the reliability of our simulation code, the differential cross section has been calculated simultaneously for the two η decays: $\eta \to 2\gamma$ and $\eta \to 3\pi^0$. The comparison at one energy (800 MeV) is displayed in Fig. 2 and illustrates the excellent agreement between both results. In addition, we have systematically used the high statistics reaction $p(\gamma, \pi^0 p)$ to perform precise tests and comparisons with

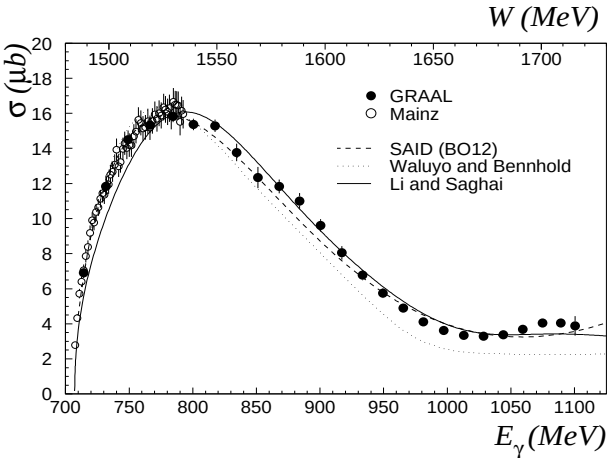

Fig. 3. Total cross section of the $p(\gamma, \eta p)$ reaction. The GRAAL results (close circles) are compared with previous experimental results and to three different analyses. See text for details.

the world data base [16]. The error bars shown in the data correspond to the quadratic sum of all systematic and statistical errors except for those due to global normalisation factors estimated to be $\pm 3.0\%$.

The total cross section has been obtained by integration of the differential cross section, using a polynomial fit in $\cos\theta$ to extrapolate to the unmeasured region ($\simeq$10%). A good reduced χ^2 is already achieved with a polynomial of degree two in agreement with the smooth behavior observed in our measurements. It should be noticed that this extrapolation procedure is a source of error that cannot be evaluated experimentally.

The total cross section calculated from threshold to 1100 MeV is plotted in Fig. 3. One can notice the nice agreement with previous measurements obtained at Mainz [7] except for a small discrepancy around 800 MeV.

As mentioned earlier, the $S_{11}(1535)$ resonance strongly dominates η photoproduction up to 900 MeV and its parameters (mass, width and photocoupling amplitude) can be directly estimated from the shape of the total cross section. A fit with a single Breit-Wigner shape limited to energies less than 900 MeV gives M=1543$\pm$2 MeV and Γ_R=174$\pm$8 MeV for the mass and width of the resonance. Extending the fit to higher energies results in a much smaller width (for instance, $\Gamma_R = 152 \pm 4$ MeV for $E_\gamma \leq 950$ MeV) and underlines the presence of other contributions. Our extracted Γ_R is significantly smaller than the one obtained with the Mainz data ($\geq$200 MeV) [7] but is in agreement with the PDG estimate (150 MeV) and also with two recent electroproduction experiments performed at JLab ($\Gamma_R \approx 150$ MeV) [19,20]. The helicity amplitude $A_{1/2}$ can be readily obtained from the maximum of the cross section. It shows less sensitivity to the energy range covered but is correlated to the branching

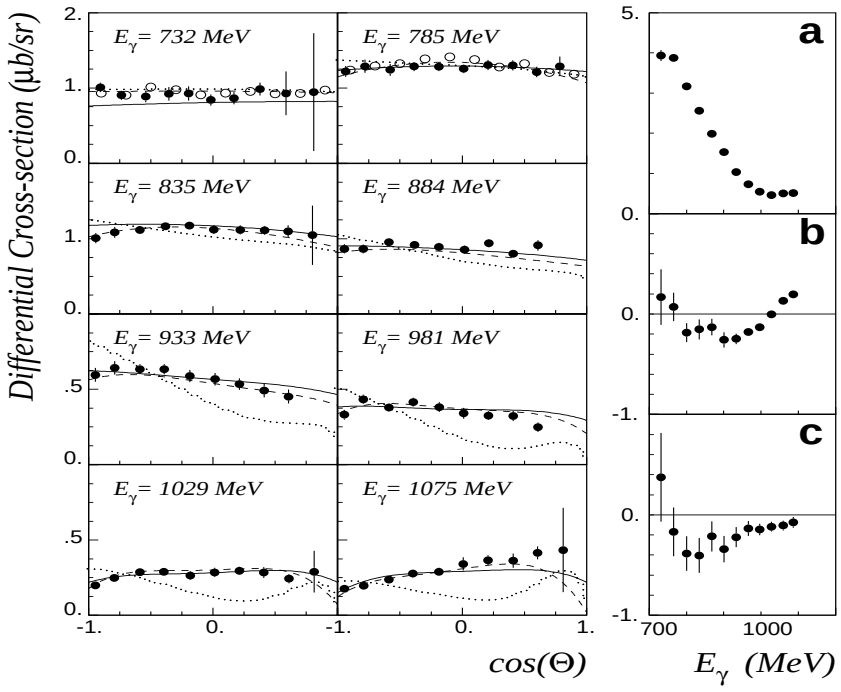

Fig. 4. Differential cross section for the $p(\gamma,\eta p)$ reaction. Legend as in Fig. 3. The coefficients a, b and c result from the fit to the data by expression (1).

ratio of the resonance to the ηp channel, b_η. Taking b_η=0.55 for consistency with extractions from the two JLab electroproduction experiments, we obtain $A_{1/2}$=102±2 10^{-3} GeV$^{-1/2}$. This value falls within the broad range of the PDG estimate (90 ± 30), but, taking into account other contributions, especially the second $S_{11}(1650)$, might significantly change the result.

The differential cross section, plotted in Fig. 4 for a sample of photon energies as a function of $\cos\theta$ where θ is the η C.M. polar angle, was measured every 17 MeV between threshold and 1100 MeV (233 points). For the two lowest energies of the figure, data from Mainz are also shown and illustrate again the good agreement between both experiments. Thanks to the overwhelming dominance of the $S_{11}(1535)$ resonance, the differential cross section can be expanded in terms of the S-wave multipole and its interference with other multipoles. Limiting the expansion to P and D waves, an approximation valid at least up to 900 MeV, the following expression can be derived [12]:

$$\frac{d\sigma}{d\Omega} = \frac{q_\eta}{k}\{a + b\,\cos\theta + c\,\cos^2\theta\} \quad (1)$$

where q_η and k are the η and γ C.M. momenta, and

$$a = |E_{0^+}|^2 - Re[E^*_{0^+}(E_{2^-} - 3M_{2^-})]$$

$$b = 2\,Re[E^*_{0^+}(3E_{1^+} + M_{1^+} - M_{1^-})]$$

$$c = 3\,Re[E^*_{0^+}(E_{2^-} - 3M_{2^-})]$$

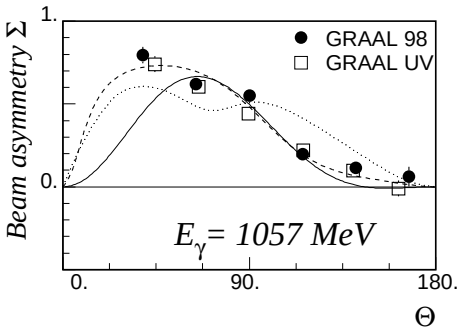

Fig. 5. Beam asymmetry Σ for the $p(\gamma, \eta p)$ reaction. Results published in 1998 (circles) are compared to new results obtained with a UV line (squares). Legend as in Fig. 3

We have fitted our results with expression (1) and the extracted coefficients are plotted versus γ-ray energy on the right-hand side of Fig. 4. As expected, the $D_{13}(1520)$ contribution already seen in ref. [7] close to threshold is observed in c (S-D interference). The b coefficient (S-P interference) exhibits small and negative values below 1000 MeV and then a sudden rise with a zero-crossing at E_γ=1030 MeV (W=1680 MeV), which indicates the onset of a P-wave. A similar trend has been observed in electroproduction at low Q^2 [20] where this P-wave has been associated with the $P_{11}(1710)$ resonance. Above 1000 MeV, nevertheless, a simple interpretation of these coefficients becomes doubtful since S-wave dominance vanishes.

A multipole analysis has been performed by the GWU group [21]. They achieved a nice global fit to the cross section (dashed line, Figs. 3 and 4) and asymmetry (Fig. 5); for the latter, we have displayed the highest energy bin published in 1998 and a new measurement using a UV laser line that confirms the large values at forward angle. Only S, P and D multipoles are needed; this rules out a strong contribution from the $F_{15}(1680)$. Analysis of the individual multipoles confirms the previous qualitative conclusions and indicates strong P and D-wave contributions above 900 MeV. These higher multipoles can indeed be associated with nucleon resonances ($P_{11}(1710)$ or $P_{13}(1720)$, $D_{15}(1675)$ or $D_{13}(1700)$), but additional contributions can originate from vector meson exchange as well as nucleon Born terms. In order to start exploring this new domain, we present below preliminary results of two models which bring different answers to this question.

The first, from Waluyo and Bennhold, [22,23] is a coupled-channel calculation based on the Bethe-Salpeter equation in the K-matrix approximation. It includes all hadronic and electromagnetic reactions with γN, πN, $\pi\pi$N, ηN, KΛ, KΣ and η'N asymptotic states. Nucleon resonances with spin J $\leq 3/2$ are included up to M = 2 GeV. The results, based on a large data base, are plotted in Figs. 3 to 5 (dotted line). They show fair overall agreement, especially for Σ, and to a lesser extent for $d\sigma/d\Omega$, in particular at high energy.

Their unexpected conclusion is that above 900 MeV, the forward peaking of Σ is primarily due to intermediate vector meson exchange in the t-channel.

The second, from Li and Saghai, [10,24] is based on a quark model and includes all known resonances. To avoid double counting, vector meson exchange in the t-channel is excluded, a valid approximation as long as resonant contributions dominate. An interesting property of this approach is that it directly links data to the quark model, hence to quantities such as mixing angles of resonance configurations [25]. The model, constrained by our data only, is able to reproduce rather well the global trend for the cross section (full curve), although significant deviations are observed near threshold and above 1000 MeV. The shape of the beam asymmetry is also fairly well reproduced but, despite its contribution, the $F_{15}(1680)$ cannot explain the forward peaking. In their most recent analysis [26], the authors have shown that, thanks to the inclusion of a new S_{11} resonance around 1700 MeV, they obtain a significant improvement and are now able to reproduce nicely the set of data, except the forward asymmetry at 40^0 and 1057 MeV.

In summary, we have measured the differential cross section for the reaction $p(\gamma, \eta p)$ from threshold to 1100 MeV photon lab. energy, completing our previous measurement of the beam asymmetry Σ over the same energy range. Below 900 MeV, the reaction mechanism is well understood and these data will contribute to a precise determination of the dominant $S_{11}(1535)$ parameters. Above this energy, S-wave dominance vanishes and the data show a rapid transition to a new regime with a clear P-wave contribution. It seems established that the $F_{15}(1680)$ resonance is not the main source of the forward peaking observed in Σ. We are looking forward to definitive analyses that will allow the extraction of as yet unknown couplings of baryon resonances to the η meson.

Acknowledgements

We are grateful to C. Bennhold, B. Saghai and I. Strakovsky for helpful discussions and communication of their analyses prior to publication. It is a pleasure to thank the ESRF for the reliable and stable operation of the storage ring and the technical staff of the contributing institutions for essential help in the realization and maintenance of the apparatus.

References

[1] For a recent review, see T.P. Vrana, S.A. Dytman, T.S.H. Lee, Phys. Rep. **328** (2000) and references therein.

[2] Review of Part. Phys., Eur. Phys. J. **C15**, 1-878 (2000).

[3] Models of the nucleon, R.K. Bhaduri (Addison Wesley, 1988).

[4] S. Capstick and W. Roberts, Phys. Rev. **D47**, 1994 (1993); Phys. Rev. **D49**, 4570 (1994).

[5] R.A. Arndt, I.I. Strakovsky and R.L. Workman, Phys. Rev. **C56**, 577 (1997).

[6] D. Drechsel, O. Hanstein, S.S. Kamalov and L. Tiator, Nucl. Phys. **A645**, 145 (1999).

[7] B. Krusche *et al.*, Phys. Rev. Lett. **74**, 3736 (1995).

[8] A. Bock *et al.*, Phys. Rev. Lett. **81**, 534 (1998).

[9] J. Ajaka *et al.*, Phys. Rev. Lett. **81**, 1797 (1998).

[10] Z. Li and B. Saghai, Nucl. Phys. **A644**, 345 (1998).

[11] N. Mukhopahyay and N. Mathur, Phys. Lett. **B444**, 7 (1998).

[12] L. Tiator, D. Drechsel, G. Knochlein, C. Bennhold, Phys. Rev. **C60**, 035210 (1999).

[13] R. Workman, R.A. Arndt, I. Strakovsky, Phys. Rev. **C62**, 048201 (2000).

[14] P. Levi Sandri *et al.*, Nucl. Inst. Meth. **A370**, 396 (1996).

[15] D. Barancourt *et al.*, Nucl. Inst. Meth. **A388**, 226 (1997).

[16] F. Renard, Thesis, Univ. J. Fourier (Grenoble, 1999), available upon request.

[17] J. Ajaka *et al.*, Phys. Lett. **B475**, 372 (2000).

[18] L. Mazzaschi *et al.*, Nucl. Inst. Meth. **A436**, 441 (1994).

[19] C.S. Armstrong *et al.*, Phys. Rev. **D60**, 052004 (1999).

[20] R. Thompson *et al.*, Phys. Rev. Lett. **86**, 1702 (2001).

[21] R.A. Arndt, I.I. Strakovsky and R.L. Workman, BAPS **45**, 43 (2000) and private communication.

[22] A. Waluyo and C. Bennhold, private communication.

[23] C. Bennhold *et al.*, nucl-th/9901066, nucl-th/0008024, T. Feuster and U. Mosel, Phys. Rev. **C59**, 460 (1999).

[24] B. Saghai, private communication.

[25] B. Saghai, N*2000 Workshop Proceedings (to appear in World Scientific), JLab (2000).

[26] B. Saghai and Z. Li, Eur. Phys. J. A **11**,217 (2001).